

## Probing the Channel-Bound *Shaker* B Inactivating Peptide by Stereoisomeric Substitution at a Strategic Tyrosine Residue<sup>†</sup>

J. A. Encinar,<sup>‡</sup> A. M. Fernández,<sup>‡</sup> J. A. Poveda,<sup>‡</sup> M. L. Molina,<sup>‡</sup> J. P. Albar,<sup>§</sup> F. Gavilanes,<sup>||</sup> and J. M. Gonzalez-Ros<sup>\*‡</sup>

*Instituto de Biología Molecular y Celular, Universidad Miguel Hernández, Elche, 03202 Alicante, Spain, Centro Nacional de Biotecnología, CSIC, Departamento de Inmunología y Oncología, Cantoblanco, 28049 Madrid, Spain, and Departamento de Bioquímica, Facultad de Ciencias Químicas, Universidad Complutense, 28040 Madrid, Spain*

Received February 24, 2003; Revised Manuscript Received May 6, 2003

**ABSTRACT:** A synthetic peptide patterned after the sequence of the inactivating ball domain of the *Shaker* B K<sup>+</sup> channel, the ShB peptide, fully restores fast inactivation in the deletion *Shaker* BΔ6–46 K<sup>+</sup> channel, which lacks the constitutive ball domains. On the contrary, a similar peptide in which tyrosine 8 is substituted by the secondary structure-disrupting D-tyrosine stereoisomer does not. This suggests that the stereoisomeric substitution prevents the peptide from adopting a structured conformation when bound to the channel during inactivation. Moreover, characteristic *in vitro* features of the wild-type ShB peptide such as the marked propensity to adopt an intramolecular β-hairpin structure when challenged by anionic phospholipid vesicles, a model target mimicking features of the inactivation site in the channel protein, or to insert into their hydrophobic bilayers, are lost in the D-tyrosine-containing peptide, whose behavior is practically identical to that of noninactivating peptide mutants. In the absence of high resolution crystallographic data on the inactivated channel/peptide complex, these latter findings suggest that the structured conformation required for the peptide to promote channel inactivation, as referred to above, is likely to be β-hairpin.

Fast (N-type) inactivation of voltage-activated potassium (K<sub>v</sub>)<sup>1</sup> (*I*) channels occurs by a ball and chain mechanism in which a flexible N-terminal domain (the ball or inactivation gate), which is either part of the channel protein (α-subunit) itself or forms part of an accompanying β-subunit, acts as an open channel blocker and physically occludes the cytoplasmic channel mouth (*1, 2*). In the *Shaker* B K<sub>v</sub> channel (*3*), the inactivating ball domain corresponds to the first 20 amino acids in the N-terminal region of each of the four *Shaker* B channel α-subunits (H<sub>2</sub>N-MAAVAGLYGLGE-DRQHRKKQ). These *Shaker* B ball domains behave independently (*4, 5*), each causing channel inactivation in a mutually exclusive manner.

Following the identification of the ball domain in the *Shaker* B K<sup>+</sup> channel, it was found that intracellular addition of a synthetic peptide (the ShB inactivating peptide) patterned after the ball sequence fully restores fast inactivation in

mutant *Shaker* B channels that do not inactivate because of deletions in their N-terminal region, suggesting that the synthetic peptide contains all the necessary molecular determinants to recognize the channel protein and restore inactivation (*6*). The notion that fragments of membrane proteins can often retain their structure and function in the absence of an intact peptide backbone has been reviewed recently (*7*). Furthermore, the ShB inactivating peptide serves also as an inactivating ball for a variety of other K<sub>v</sub> channels (*6, 8, 9*), high- and intermediate-conductance, Ca<sup>2+</sup>-activated K<sup>+</sup> channels (*10–12*), or cyclic nucleotide-gated channels (*13*), some of which do not inactivate physiologically. From the above observations, it was concluded that the molecular recognition events leading to the formation of the inactivating peptide/channel complex, and thus to channel inactivation, have a rather unconstrained basis in terms of primary structure and that there must be two relevant domains, complementary to those in the ball peptides, configuring the site for the inactivating peptide in the channel protein: (i) a hydrophobic pocket, which becomes accessible only upon channel opening, separated from the cytoplasm by (ii) a region with a negative surface potential (*14–16*). Such conclusions received support from the crystal structure of the prokaryotic KcsA and MthK channels (*17–19*) in which the central cavity and inner channel pore are lined by hydrophobic amino acids, while the surrounding cytoplasmic domains contain plenty of acidic amino acids to favor electrostatic interaction with the positively charged amino acids found near the C-terminus in most ball peptides.

<sup>†</sup> Partly supported by grants from the Spanish DGI BFI2002-03410 and BMC2000-0545.

\* To whom correspondence should be addressed. Phone: +34 96 6658757. Fax: +34 96 6658758. E-mail: gonzalez.ros@umh.es.

<sup>‡</sup> Universidad Miguel Hernández.

<sup>§</sup> Centro Nacional de Biotecnología.

<sup>||</sup> Universidad Complutense.

<sup>1</sup> Abbreviations: K<sub>v</sub>, voltage-activated potassium channels; *Shaker* B K<sup>+</sup> channel, one of the spliced-variants of the voltage-dependent, fast-inactivating K<sup>+</sup> channels coded in the *Shaker* locus of *Drosophila*; ShB peptide, inactivating peptide of the *Shaker* B K<sup>+</sup> channel; PC, phosphatidylcholine from egg yolk; PG, phosphatidylglycerol prepared from egg yolk PC; PA, phosphatidic acid prepared from egg yolk PC; DMPA, 1,2-dimyristoyl-*sn*-glycero-3-phosphate; FTIR, Fourier transform infrared spectroscopy; DSC, differential scanning calorimetry.

To date, no crystallographic data are yet available on the inactivated channel/ball peptide complex. Nevertheless, electrophysiological results from cycle mutational analysis of the interactions between a construct called the  $\beta$ -12 subunit as the inactivation gate and a mammalian homologue of *Shaker*, the  $K_v$  1.4 channel, suggest that the inactivating ball peptide snakes its way into the cytoplasmic channel mouth and stays there during inactivation in an almost linear, fully extended conformation (18). Indeed, a similar conclusion was previously reported from electrophysiological studies of inactivation peptide mutants (20). On the other hand, the conformational propensity of both the ball peptide of the  $K_v$  3.4 channel (21) as well as that of the ShB peptide (22–24) have been studied spectroscopically in the presence of anionic phospholipid vesicles that, similarly to the inactivation site on the channel protein (17–19), contain a hydrophobic domain (the lipid bilayer), separated from the aqueous media by a negatively charged surface (the vesicle surface). These latter studies have shown that the ball peptides are indeed poorly structured in solution but adopt  $\beta$ -structure when challenged by the channel-mimicking model target. Moreover, the  $\beta$ -structure adopted by the ShB peptide has been identified as a hydrophobic  $\beta$ -hairpin that readily inserts into the hydrophobic domains provided by the lipid bilayer (23, 24).

In an attempt to gain insight into the molecular events involving the inactivating peptide during channel inactivation, we are now reporting on the effects of substituting the naturally occurring L isomer of Y8 in the ShB peptide sequence by its D stereoisomer (ShB-Y8y). The rationale is that, if one assumes a fully extended conformation for the channel-bound peptide, such substitution would not be expected to change dramatically the ability of the peptide to interact with the channel, particularly considering that the channel is a homotetramer and thus, the inner pore has a 4-fold symmetry of equivalent, potential peptide binding sites. On the contrary, because of both steric hindrance by the bulky phenol ring and disruption of hydrogen bonding, the D stereoisomer substitution can be anticipated to interfere greatly with the adoption of ordered motifs of secondary structure by the channel-bound peptide (25). Our experimental observation is that the ShB-Y8y peptide loses the ability shown by the wild-type ShB peptide to induce rapid inactivation of the *Shaker* BA6–46  $K^+$  channels expressed in CHO cells; therefore, it apparently favors the hypothesis that the inactivating peptide adopts a structured conformation when bound to the channel. Moreover, when confronted *in vitro* to the anionic vesicle model target, the ShB-Y8y peptide resembles very closely the behavior of noninactivating peptide mutants since it can neither adopt the characteristic  $\beta$ -hairpin structure exhibited by the wild-type ShB peptide nor insert into the hydrophobic bilayer. These latter observations suggest that, given the conformational propensity observed in the ShB peptide, the ordered structure adopted by the ball peptide in the inactivated channel complex is likely to be a  $\beta$ -hairpin.

## MATERIALS AND METHODS

The wild-type ShB peptide and the ShB-Y8y derivative were synthesized as C-terminal amides on an automatic multiple synthesizer (AMS 422, Abimed) using a solid-phase procedure and standard Fmoc-chemistry (22). The peptides

were purified by reverse-phase HPLC to better than 95% purity, and their composition and molecular mass were confirmed by amino acid analysis and mass spectrometry, respectively (22). Residual trifluoroacetic acid used both in the peptide synthesis and in the HPLC mobile phase (the trifluoroacetate ion has a strong infrared absorbance at 1673  $\text{cm}^{-1}$ , which interferes with the characterization of the amide I band; see ref 26) was removed by submitting the peptides to several lyophilization–solubilization cycles in 10 mM HCl (27).

*Shaker* BA6–46  $K^+$  channel cDNA (3, 28) was transiently expressed in CHO cells using the p513 vector (Stratagene) (29). Cell culture and electroporation conditions were as described previously (30). Ionic currents were recorded 24–48 h after transfection, using the whole-cell configuration of the patch-clamp technique (31). Experiments were performed in cells expressing between 0.8 and 1.2 nA of peak current amplitudes at +20 mV.

The phospholipids phosphatidylglycerol (PG) and phosphatidic acid (PA) (Avanti Polar Lipids) used in the infrared spectroscopy studies derive from egg yolk PC and therefore have the same fatty acid composition. For infrared amide I band recordings, lyophilized aliquots of the synthetic peptides and the desired lipids were separately hydrated in a bath-type sonicator in 25  $\mu\text{L}$  of  $\text{D}_2\text{O}$  buffers (see figure legends for details on the composition of the buffers) to avoid the interference of  $\text{H}_2\text{O}$  infrared absorbance (1645  $\text{cm}^{-1}$ ; ref 32). The resulting solutions were mixed by placing them together into a liquid demountable cell (Harrick, Ossining, NY) equipped with  $\text{CaF}_2$  windows and 50  $\mu\text{m}$ -thick Mylar spacers and maintained at room temperature for approximately 30 min to ensure that the isotopic H–D amide proton exchange reached equilibrium, as judged by a constant minimal absorbance at the residual amide II band in the peptide's infrared spectra. The peptide concentrations in the final mixtures ranged from 1.1–4.5 mM, while the phospholipids were used at approximately 32.8 mM, thus resulting in peptide to phospholipid molar ratios ranging from 0.03 to 0.14. Infrared spectra were taken in a Nicolet 520 instrument equipped with a DTGS detector, as previously described (33), using 200 spectral scans to define the amide I band. No resolution-enhancement techniques (Fourier derivation or deconvolution) were applied to the spectral data.

For Differential Scanning Calorimetry (DSC), large multilamellar vesicles made from synthetic, dimyristoyl phosphatidic acid (DMPA) (Avanti Polar Lipids) were used. Dried lipid films obtained from chloroform solutions were suspended in the required buffer (see figure legends for details) to a final concentration of 2 mM in terms of lipid phosphorus. The suspended lipids were kept for 90 min above their phase transition temperatures and vortexed. The resulting liposomes were stored overnight, at 4  $^\circ\text{C}$ , to ensure a complete hydration of the sample prior to the DSC experiments. Thermograms were recorded on a high-resolution Microcal MC-2 differential scanning microcalorimeter, equipped with the DA-2 digital interface and data acquisition utility for automatic data collection, as described earlier (34). The lipid dispersions containing added peptides at different molar ratios and the corresponding buffer in the reference cell were thermally equilibrated in the microcalorimeter, at  $\sim 10$   $^\circ\text{C}$  during 45 min, before a temperature gradient was applied. Differences in the heat capacity between the sample and the reference

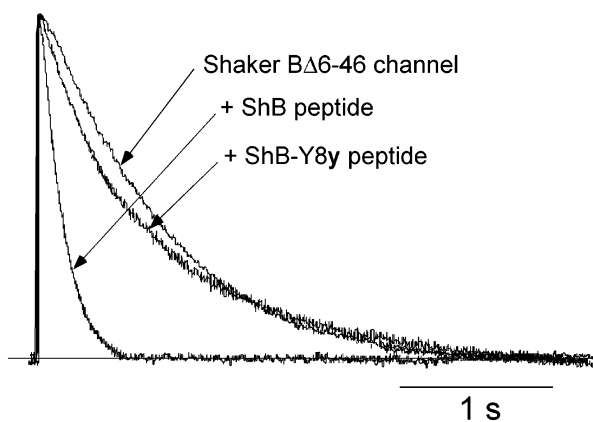


FIGURE 1: Restoration of fast (N-type) inactivation in the deletion mutant *Shaker* B $\Delta$ 6–46 K<sup>+</sup> channel. Slow (C-type) inactivation of the *Shaker* B $\Delta$ 6–46 channel in the absence of inactivating peptides is shown as a control. The figure shows the effects of the ShB and ShB-Y8y peptides on restoring fast inactivation in the *Shaker* B $\Delta$ 6–46 channel. The whole-cell configuration of the patch-clamp technique was used in these studies. The external bathing solution (pH 7.4) contained (in mM) 140 NaCl, 2.7 KCl, 2.5 CaCl<sub>2</sub>, 4 MgCl<sub>2</sub>, and 10 Hepes. The pipet solution (pH 7.2) contained (in mM) 80 KCl, 30 potassium glutamate, 20 KF, 4 MgCl<sub>2</sub>, 4 ATP, 10 EGTA, and 10 Hepes. In all cases, the peptides were dissolved in the pipet solution at a concentration of 500  $\mu$ M.

cell were obtained by raising the temperature at a constant rate of 45 °C/h. Transition temperatures and enthalpies were calculated by fitting the observed transitions to a single van't Hoff component.

## RESULTS

**Functional Effects of the ShB-Y8y Peptide on Channel Inactivation.** The ability of the synthetic ShB-Y8y peptide to restore N-type K<sup>+</sup> channel inactivation was tested by studying its effects in a *Shaker* B K<sup>+</sup> channel mutant, the *Shaker* B $\Delta$ 6–46 K<sup>+</sup> channel, in which the large deletion near its N-terminus precludes its inactivation since the constitutive ball moieties present in the wild-type *Shaker* B K<sup>+</sup> channel are missing (3, 28). Figure 1 shows representative macroscopic potassium currents elicited in response to depolarizing pulses in transfected CHO cells expressing *Shaker* B $\Delta$ 6–46 channels, both in the presence and in the absence of added peptides. Such recordings were also used to calculate the rate constants for the voltage-dependent channel activation and voltage-independent channel inactivation processes (Table 1). In the absence of inactivating peptides (control conditions, Figure 1), the macroscopic currents elicited by the *Shaker* B $\Delta$ 6–46 channel inactivate very slowly, with inactivation time constants characteristic of the C-type, slow inactivation process exhibited also by this channel (28). Figure 1 also shows that addition of the wild-type ShB peptide restores very efficiently N-type, rapid channel inactivation in the *Shaker* B $\Delta$ 6–46 channel, in agreement with previous reports from this and other laboratories (6, 30, 35). In contrast, addition of the ShB-Y8y peptide instead of the wild-type ShB peptide does not restore rapid channel inactivation, and indeed, the current recordings are very similar to those obtained from the *Shaker* B $\Delta$ 6–46 channel under control conditions, in the absence of added peptides. These results indicate that the stereoisomer substitution at Y8 in the peptide causes a significant loss in its ability to induce rapid channel inactivation, similar to that

observed for noninactivating mutants of the ShB peptide, such as the ShB-L7E peptide (6, 30).

In addition to the above, analysis of the kinetics of channel activation indicate that neither peptide alters the voltage-dependent channel activation rates, which remain practically identical to those exhibited by the *Shaker* B $\Delta$ 6–46 channel in the absence of added peptides (Table 1).

**Challenging the ShB-Y8y Peptide by Anionic Phospholipid Vesicles, a Model Target Mimicking Features of the Inactivation Site of K<sup>+</sup> Channels.** When confronted to anionic lipid vesicles as a channel-mimicking model target, the inactivating ShB peptide (i) binds through its cationic C-terminal portion to the negatively charged surface, (ii) readily adopts an intramolecular, strongly hydrogen bonded,  $\beta$ -hairpin structure, most likely defined by a  $\beta$ -turn involving residues 4–7 (VAGL) in the peptide sequence, and (iii) inserts its folded N-terminal portion into the hydrophobic bilayer (23, 24, 36). Similar experiments carried out with noninactivating, peptide mutants show that they bind also to the anionic vesicles but do not adopt the characteristic  $\beta$ -hairpin structure and have lost the ability to traverse the anionic interphase at the vesicle surface and to insert into the hydrophobic bilayer.

Figure 2 shows the infrared amide I region of spectra corresponding to the ShB and ShB-Y8y peptides in the presence of different phospholipid vesicles. When added to vesicles made from zwitterionic PC (as well as in plain aqueous buffer, in the absence of lipid vesicles), both peptides (wild type and ShB-Y8y) show a similar bell-shaped amide I band contour (traces 1 and 4) with a maximum centered at 1645 cm<sup>-1</sup>, characteristic of nonordered protein structures. Conversely, the amide I band of the two peptides differs greatly in the presence of anionic lipid vesicles made either from PA or PG. Under such conditions, the wild-type ShB peptide exhibits (traces 2 and 3) a prominent spectral component at 1623 cm<sup>-1</sup> and a smaller one at 1689 cm<sup>-1</sup> (22–24), which in this and other peptides has been related to the adoption of strongly hydrogen-bonded  $\beta$ -structures in hydrophobic environments (37). In contrast, the amide I band of the ShB-Y8y peptide, regardless of the presence of PA or PG vesicles (traces 5 and 6) stays featureless, suggesting that the peptide containing the stereoisomeric substitution remains in a nonordered conformation under these conditions. Additional experiments were carried out at different peptide concentrations and peptide-to-phospholipid ratios with essentially identical results (not shown).

In addition to folding as an intramolecular  $\beta$ -hairpin, the ability to insert into the hydrophobic bilayer is probably what distinguishes best between inactivating and noninactivating peptides in their interaction with the anionic vesicle model targets (23, 36). Figure 3 shows DSC studies at neutral pH, in which the two peptides are confronted to vesicles made from synthetic dimirystoyl phosphatidic acid (DMPA), which has a convenient gel-to-liquid crystal phase transition temperature at 49.6 °C. As reported previously (23, 35), presence of the native, channel inactivating ShB peptide causes a large, concentration-dependent decrease in the transition enthalpy, without modifying significantly the phase transition temperature. This is due to peptide insertion into the bilayer (24, 36) in which the interaction of the peptide with the phospholipid acyl chains prevents part of the phospholipid molecules from undergoing the phase transition characteristic

Table 1: Effect of the Wild-Type ShB Peptide and of the ShB-Y8y Derivative on the Rates of Activation and Inactivation of *Shaker* BΔ6–46 K<sup>+</sup> Channel Currents<sup>a</sup>

| peptide                 | $t_{1/2}$ activation (ms) <sup>b</sup> |                 |                 | $\tau$ inactivation (ms) <sup>c</sup> |
|-------------------------|--|-----------------|-----------------|---------------------------------------|
|                         | –20 mV                                 | 0 mV            | +20 mV          | +20 mV                                |
| control<br>(no peptide) | 5.63 ± 1.12 (7)                        | 3.28 ± 0.43 (8) | 2.32 ± 0.21 (8) | 1300 ± 160 (6)                        |
| ShB                     | 4.91 ± 0.95 (5)                        | 3.17 ± 0.39 (7) | 2.22 ± 0.23 (6) | 215 ± 48 (6)                          |
| ShBY8y                  | 5.18 ± 1.19 (4)                        | 3.51 ± 0.53 (4) | 2.35 ± 0.33 (4) | 802 ± 99 (5)                          |

<sup>a</sup> Data represent mean ± standard deviation of the number of experiments indicated in parentheses. Time is given in milliseconds. Holding potential was –80 mV. <sup>b</sup> Activation kinetics are compared by measuring the time needed to reach 50% of the maximal current amplitude ( $t_{1/2}$ ) at –20, 0, and +20 mV. <sup>c</sup> Inactivation time course is studied by measuring the time needed to remain 1/e of the maximal current amplitude ( $\tau$  inactivation) at +20 mV.  $\tau$  inactivation was estimated from single-exponential fits to the current traces.

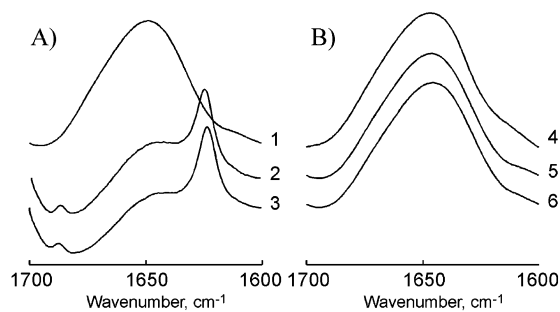


FIGURE 2: Amide I band region of the original infrared spectra of the ShB (A) and ShB-Y8y (B) peptides in the presence of PC (1, 4), PA (2, 5), and PG (3, 6) lipid vesicles. The samples were suspended in a D<sub>2</sub>O media prepared from 10 mM Hepes buffer, pD 7.4, containing 130 mM KCl and 20 mM NaCl (pD = pH + 0.4). All spectra were taken at 20 °C. A peptide/phospholipid molar ratio of 0.14 was used in these experiments.

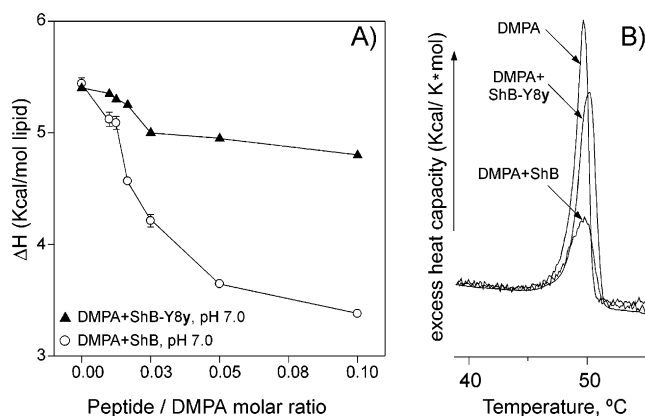


FIGURE 3: (A) Changes in the apparent gel to liquid crystal phase transition enthalpies of DMPA large multilamellar vesicles in the presence of increasing concentrations of either ShB (o) or ShB-Y8y (▲) peptides, as determined by differential scanning calorimetry of the indicated peptide–phospholipid mixtures in 10 mM Hepes, pH 7.0, 100 mM NaCl. Error bars represent standard deviations. (B) Representative DSC thermograms for the DMPA vesicles/peptide mixtures from above. The phospholipid concentration in these samples was 1 mM, and the peptide/phospholipid molar ratio was 0.10. The thermograms shown correspond to pure DMPA, in the absence of any peptide, and to DMPA vesicles in the presence of identical amounts of ShB and ShBY8y peptides.

of the pure phospholipid species, and thus decreases the apparent phase transition enthalpy in a peptide concentration-dependent manner (38). On the contrary, the ShB-Y8y peptide does not significantly affect either the apparent phase transition enthalpy or the phase transition temperature exhibited by the DMPA vesicles, even at high peptide concentration (Figure 3). This behavior of the ShB-Y8y peptide should be interpreted as being unable to insert into

the hydrophobic bilayer provided by the DMPA vesicles and resembles very closely that exhibited by the mutant, noninactivating ShB-L7E peptide (24, 36).

## DISCUSSION

The Y8 residue at the inactivating ShB peptide sequence is not strictly required for channel inactivation, as the conservative Y8F mutation still retains the ability to inactivate the channel (20). Nonetheless, introduction of a net charge at Y8, such as that resulting from tyrosine phosphorylation (35), leads to a peptide unable to induce inactivation, similar to the well-known ShB-L7E noninactivating peptide mutant (6). Y8 is also near the  $\beta$ -fold of the  $\beta$ -hairpin formed in response to challenge by anionic lipid vesicles (24); thus, it is a strategic site to probe structure/function relations in the ShB peptide.

We report here that substituting Y8 in the ShB peptide by its D stereoisomer causes an almost complete loss in its ability to restore rapid inactivation of the *Shaker* BΔ6–46 K<sup>+</sup> channel. This is accompanied by the observations that the ShB-Y8y peptide is no longer able to adopt the characteristic  $\beta$ -hairpin structure exhibited by the wild-type ShB peptide when challenged by anionic lipid vesicles or to insert into the hydrophobic bilayer of such vesicles. As previously suggested, these changes in structure and function seen in noninactivating mutants of the ShB peptide might be related by cause and effect, as it seems that an adequate folding (canceling net charges and compensating polar interactions) (24) causes the N-terminal half of the inactivating peptide to become sufficiently hydrophobic as to readily insert into the hydrophobic bilayer of the model target, or tentatively, into the hydrophobic cytoplasmic mouth of the channel pore.

Substitution of an amino acid residue by its D stereoisomer in a polypeptide chain induces profound changes in the spatial location and orientation of chemical groups and side chains involved in hydrogen bonding, van der Waals interactions, salt bridge formation, and other forces responsible for maintaining secondary and tertiary structure motifs (25). In our case, being a tyrosine that is the residue involved, steric hindrance on such structural motifs caused by spatial relocation of the bulky phenol ring should also be taken into account. Thus, it seems reasonable to interpret the above experimental observations to conclude that the channel-bound ShB peptide adopts an ordered secondary structure, which becomes disabled in the ShB-Y8y peptide. Moreover, based on the strong conformational propensity of the inactivating ShB peptide when confronted to anionic lipid vesicles (22–24), which is also observed in the ball peptide of the K<sub>v</sub> 3.4

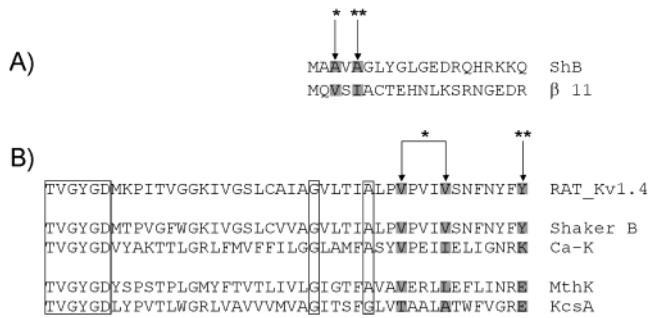


FIGURE 4: Sequence analysis of different domains of potassium channels. (A) N-terminal sequences of the *Shaker* B and rat  $\beta$ 1.1-subunit inactivating ball domains. (B) Sequences of the selectivity filters and pore-lining transmembrane segments of rat Kv1.4 (P15385), *Shaker* B (P08510), potassium large conductance, calcium-activated (Q9R196), MthK (O27564), and KcsA (Q54397) channels. The boxes indicate, from left to right, the selectivity filter, the gating hinge glycine, and the amino acid at the narrowest point of the MthK intracellular pore entryway or its equivalent residue in the other channels, respectively. The signs (\*) and (\*\*) on the channel and ball domain sequences indicate the positions of proposed coupled residues, according to the cycle mutational analysis reported by Zhou et al. (18). Numbers in parentheses following each channel's name are SWISS-PROT access numbers.

channel (21), it seems reasonable to assume that the structure adopted by the inactivating peptides during channel inactivation is likely a  $\beta$ -hairpin.

Despite great advances in the crystallographic structure of potassium channels (17–19), structural information on the inactivated channel to corroborate the above hypothesis is still lacking. In the absence of such direct information and besides the already mentioned reports using the anionic lipid vesicles as channel-mimicking model targets, other relevant data come from a double-mutant cycle analysis (18) using the  $\alpha$ -subunit of rat  $K_v$  1.4 channel, a mammalian homologue of *Shaker*, coexpressed in *Xenopus* oocytes with the construct  $\beta$ -12 subunit as the inactivation gate. Electrophysiological analysis of kinetic parameters in double mutants (i.e., a point mutation to alanine in the channel and another one in the gate) allows for the calculation of a coupling parameter,  $\Omega$ , which is taken as indicative of physical proximity between the two mutated sites. The data from Zhou and co-workers show that both V558 and V562 in the  $K_v$  1.4 channel are coupled to V3 in the gate, while Y569 in the channel is coupled to I5 in the gate (Figure 4). On the basis of these data, the interpretation given by the authors is that the inactivation gate lies in the inner channel pore and in a fully extended conformation. Figure 4 also compares the sequence of the  $\beta$ -12 gate with that of the inactivating ShB peptide. The comparison shows that V3 and I5 in the  $\beta$ -12 gate correspond to A3 and A5 in the ShB peptide, suggesting that rather than specific amino acids, the residues in the inactivation peptides coupled to those in the  $K_v$  1.4 channel referred above must be of a hydrophobic nature. Likewise, Figure 4 shows a sequence alignment of different potassium channels to illustrate that V558 and V562 in the  $K_v$  1.4 channel correspond either to identical or to similarly hydrophobic amino acids in channels as different as the *Drosophila Shaker* (V473 and V477) or the mammalian large conductance  $Ca^{2+}$ -activated  $K^+$  channel (V319 and I323), as well as in the prokaryotic KcsA or MthK channels (T107 and A111 or V91 and L95, respectively). All channels mentioned (except MthK, from which there is still no

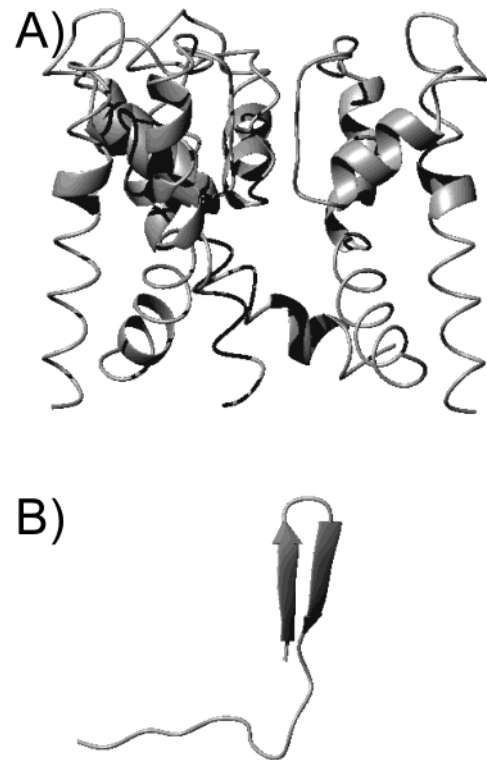


FIGURE 5: ShB inactivating peptide fits into the open pore cavity of  $K^+$  channels. The crystal structure of the MthK channel (19–98 sequence of the MthK channel, as in Protein Data Bank 1LNQ) has been taken as the open pore cavity of  $K^+$  channels. Only three out of the four identical subunits of the MthK channel have been drawn, oriented with the extracellular surface upward (A). The cytoplasmic open channel vestibule appears as a truncated cone-like cavity large enough to accommodate the ShB inactivating peptide, modeled as an intramolecular  $\beta$ -hairpin (B). This figure was prepared by using MolMol software.

reported evidence) can undergo rapid inactivation induced by the ShB peptide, and then, the observed conservation of hydrophobic residues in the inactivation binding site seems to make sense. In contrast, the coupled Y569 is not conserved at all, being also tyrosine (Y485) in *Shaker* B, but neither is lysine (K330) in the large conductance  $Ca^{2+}$ -activated  $K^+$  channel or glutamic acid (E118 or E102, respectively) in both prokaryotic KcsA or MthK channels. Such lack of conservation at those positions equivalent to Y569 in the  $K_v$  1.4 channel indicates that either the coupling assignment is wrong, possibly because of a lack of sufficient resolution of the electrophysiological technique in providing the structural information demanded, or else the site is extremely flexible and accommodates almost any kind of amino acid residues regardless of their chemical nature. In any case, the coupling that seems to hold from extending Zhou's mutational analysis to the sequences shown in Figure 4 refers to that between V558 and V562 in the  $K_v$  1.4 channel and V3 in the inactivation gate or their equivalent residues in the other sequences. Such a condition can obviously be met by assuming a fully extended conformation of the channel-bound inactivating peptide, as in Zhou's paper, but it could also be met by other possible conformations of the channel-bound inactivating peptide, such as the  $\beta$ -hairpin we postulated in the previous paragraph. This hypothetical alternative fully meets the predictions from the studies using the phospholipid vesicle model target. Moreover, the width of such a  $\beta$ -hairpin would not exceed either the size of the cytoplasmic mouth

of open potassium channels (19) (Figure 5) or the size of tetrabutylammonium or tetrabutylantimony, quaternary amines known to act as open channel blockers by entering into the hydrophobically lined channel inner pore (18). More importantly in regard to this work, the  $\beta$ -hairpin proposal explains the results obtained in trying to promote inactivation of the *Shaker* B $\Delta$ 6–46 K<sup>+</sup> channel by the ShB-Y8y peptide: D-tyrosine in the peptide chain relocates the bulky phenol ring between the two potential  $\beta$ -strands, preventing both hydrogen bonding and the adoption of the  $\beta$ -hairpin conformation and thus making the peptide unable to enter the channel inner pore and induce inactivation.

## ACKNOWLEDGMENT

We gratefully acknowledge our colleagues Drs. José López-Barneo and Antonio Molina for their help in the electrophysiological recordings of channel inactivation at the Universidad de Sevilla, Spain. We also thank Drs. J. L. Neira and J. Gómez from this Institute for their critical reading and suggestions on this manuscript.

## REFERENCES

- Armstrong, C. M., and Bezanilla, F. (1977) *J. Gen. Physiol.* 70, 567–590.
- Antz, C., and Fakler, B. (1998) *News Physiol. Sci.* 13, 177–182.
- Hoshi, T., Zagotta, W. N., and Aldrich, R. W. (1990) *Science* 250, 533–538.
- MacKinnon, R., Aldrich, R. W., and Lee, A. W. (1993) *Science* 262, 757–759.
- Gomez-Lagunas, F., and Armstrong, C. M. (1995) *Biophys. J.* 68, 89–95.
- Zagotta, W. N., Hoshi, T., and Aldrich, R. W. (1990) *Science* 250, 568–571.
- Shai, Y. (2001) *J. Membr. Biol.* 182, 91–104.
- Isacoff, E. Y., Jan, Y. N., and Jan, L. Y. (1991) *Nature* 353, 86–90.
- Dubinsky, W. P., Mayorka-Wark, O., and Schultz, S. (1992) *Proc. Natl. Acad. Sci. U.S.A.* 89, 1770–1774.
- Toro, L., Stefani, E., and LaTorre, R. (1992) *Neuron* 9, 237–245.
- Foster, C. D., Chung, S., Zagotta, W. N., Aldrich, R. W., and Levitan, I. B. (1992) *Neuron* 9, 229–236.
- Riquelme, G., Fernández, A. M., Encinar, J. A., Gonzalez-Ros, J. M., and Sepúlveda, F. V. (1999) *Pflugers Arch.* 438, 879–882.
- Kramer, R. H., Goulding, E., and Siegelbaum, S. A. (1994) *Neuron* 12, 655–662.
- Jan, L. Y., and Jan, Y. N. (1992) *Annu. Rev. Physiol.* 54, 537–555.
- Catterall, W. A. (1995) *Annu. Rev. Biochem.* 64, 493–531.
- Kukuljan, M., Labarca, P., and LaTorre, R. (1995) *Am. J. Physiol. Cell Physiol.* 268, C535–C556.
- Doyle, D. A., Morais-Cabral, J., Pfuetzner, R. A., Kuo, A., Gulbis, J. M., Cohen, S. L., Chait, B. T., and MacKinnon, R. (1998) *Science* 280, 69–77.
- Zhou, M., Morais-Cabral, J. H., Mann, S., and MacKinnon, R. (2001) *Nature* 411, 657–661.
- Jiang, Y., Lee, A., Chen, J., Cadene, M., Chait, B. T., MacKinnon, R. (2002) *Nature* 417, 515–522.
- Murrell-Lagnado, R. D., and Aldrich, R. W. (1993) *J. Gen. Physiol.* 102, 949–975.
- Abbott, G. W., Mercer, E. A., Miller, R. T., Ramesh, B., and Srani, S. K. (1998) *Biochemistry* 37, 1640–1645.
- Fernández-Ballester, G., Gavilanes, F., Albar, J. P., Criado, C., Ferragut, J. A., and González-Ros, J. M. (1995) *Biophys. J.* 68, 858–865.
- Encinar, J. A., Fernández, A. M., Gavilanes, F., Albar, J. P., Ferragut, J. A., and González-Ros, J. M. (1996) *Biophys. J.* 71, 1313–1323.
- Encinar, J. A., Fernández, A. M., Gil-Martín, E., Gavilanes, F., Albar, J. P., Ferragut, J. A., and Gonzalez-Ros, J. M. (1998) *Biochem. J.* 331, 497–504.
- Hong, S. Y., Oh, J. E., and Lee, K.-H. (1999) *Biochem. Pharmacol.* 58, 1775–1780.
- Surewicz, W. K., Mantsch, H. H., and Chapman, D. (1993) *Biochemistry* 32, 389–394.
- Zhang, Y.-P., Lewis, R. N. A. H., Hodges, R. S., and McElhaney, R. N. (1992) *Biochemistry* 31, 11572–11578.
- López-Barneo, J., Hoshi, T., Heinemann, S. H., and Aldrich, R. W. (1993) *Recept. Channels* 1, 61–71.
- Green, S., Issemann, J., and Sher, E. (1988) *Nucleic Acid Res.* 16, 369.
- Fernández, A. M., Molina, A., Encinar, J. A., Gavilanes, F., López-Barneo, J., and González-Ros, J. M. (1996) *FEBS Lett.* 398, 81–86.
- Hamill, O. P., Marty, A., Neher, E., Sakmann, B., and Sigworth, F. J. (1981) *Pflugers Arch.* 391, 85–100.
- Mendelsohn, R., and Mantsch, H. H. (1986) in *Progress in Protein-Lipid Interactions*, Watts, A. and DePont, A., Eds., pp 103–146, Elsevier Science B. V., Amsterdam.
- Castresana, J., Fernández-Ballester, G., Fernández, A. M., Laynez, J. L., Arrondo, J. L. R., Ferragut, J. A., and González-Ros, J. M. (1992) *FEBS Lett.* 314, 171–175.
- Villar, M. T., Artigues, A., Ferragut, J. A., and González-Ros, J. M. (1988) *Biochim. Biophys. Acta* 938, 35–43.
- Encinar, J. A., Fernández, A. M., Molina, M. L., Molina, A., Poveda, J. A., Albar, J. P., Lopez-Barneo, J., Gavilanes, F., Ferrer-Montiel, A. V., and Gonzalez-Ros, J. M. (2002) *Biochemistry* 41, 12263–12269.
- Poveda, J. A., Prieto, M., Encinar, J. A., González-Ros, J. M., and Mateo, C. R. (2003) *Biochemistry*, in press.
- Demel, R. A., Goormaghtigh, E., and de Kruijff, B. (1990) *Biochim. Biophys. Acta* 1027, 155–162.
- Papahadjopoulos, D., Moscarello, M., Eylar, E. H., and Isac, T. (1975) *Biochim. Biophys. Acta* 401, 317–335.

BI0343121